JOURNAL OF FLUIDS AND STRUCTURES

Journal of Fluids and Structures 23 (2007) 649–663

www.elsevier.com/locate/jfs

Linear water wave propagation through multiple floating elastic plates of variable properties

A.L. Kohout[a], M.H. Meylan[a,*], S. Sakai[b], K. Hanai[b], P. Leman[a], D. Brossard[a]

[a]Department of Mathematics, University of Auckland, Private Bag 92019, Auckland, New Zealand
[b]Department of Civil Engineering, Iwate University, Morioka, Japan

Received 11 April 2006; accepted 25 October 2006
Available online 8 January 2007

Abstract

We investigate the problem of linear water wave propagation under a set of elastic plates of variable properties. The problem is two-dimensional, but we allow the waves to be incident from an angle. Since the properties of the elastic plates can be set arbitrarily, the solution method can also be applied to model regions of open water as well as elastic plates. We assume that the boundary conditions at the plate edges are the free boundary conditions, although the method could be extended straightforwardly to cover other possible boundary conditions. The solution method is based on an eigenfunction expansion under each elastic plate and on matching these expansions at each plate boundary. We choose the number of matching conditions so that we have fewer equations than unknowns. The extra equations are found by applying the free-edge boundary conditions. We show that our results agree with previous work and that they satisfy the energy balance condition. We also compare our results with a series of experiments using floating elastic plates, which were performed in a two-dimensional wave tank.

Keywords: Linear water wave theory; Elastic plates; Eigenfunction expansion

1. Introduction

The study of linear wave propagation through a region of water containing floating elastic plates has been the subject of significant research. The original motivation for this study was to understand wave propagation in ice-covered seas, but recently the construction (or proposed construction) of very large floating structures (VLFS) has motivated much of the research. The research motivated by ice-covered seas is described in Squire et al. (1995) and Wadhams (2000), and the research motivated by VLFS is described in Kashiwagi (2000) and Watanabe et al. (2004).

The specific problem we are concerned with here is a two-dimensional fluid covered by a finite number of elastic plates, of possibly different properties. Within this formulation we consider regions of open water as arising from limiting cases of plates of vanishing thickness. These kinds of problems have generally been studied in the context of two semi-infinite plates (or possibly a single semi-infinite plate and open water). The simplest problem to consider is one where there are only two semi-infinite plates of identical properties separated by a crack. A simpler but related problem

*Corresponding author.
E-mail addresses: akohout@math.auckland.ac.nz (A.L. Kohout), meylan@math.auckland.ac.nz (M.H. Meylan), sakai@iwate-u.ac.jp (S. Sakai).

0889-9746/$ - see front matter
doi:10.1016/j.jfluidstructs.2006.10.012

in acoustics was considered by Kouzov (1963), who used an integral representation of the problem to solve it explicitly using the Riemann–Hilbert technique. Recently the crack problem has been considered by Squire and Dixon (2000) and by Williams and Squire (2002), using a Green function method applicable to infinitely deep water, and they obtained simple expressions for the reflection and transmission coefficients. Squire and Dixon (2001) extended the single crack problem to a multiple crack problem, in which the semi-infinite regions are separated by a region consisting of a finite number of plates of finite size with all plates having identical properties. This problem is very close to the one considered here, except that we allow the plate properties to be arbitrary. Evans and Porter (2003) considered the multiple crack problem for finitely deep water and they derived a simple solution, again in the case where all plates have identical properties. They simplified their method further and provided an explicit solution, in Porter and Evans (2006).

In parallel to the crack problem, the more challenging problem of two semi-infinite plates of different properties was considered. The first significant work on this problem was by Evans and Davies (1968), who present a solution method for evaluating the transmission and reflection of waves, in finitely deep water, propagating from a semi-infinite region of open water into a semi-infinite region of a floating elastic plate. The method of solution was based on the Wiener–Hopf technique. However, Evans and Davies (1968) found explicit solutions for the case of shallow water, and they only presented the formulation for the finite-depth water case and were not able to compute the coefficients for the reflection and transmission. This problem was solved numerically by Fox and Squire (1994) using eigenfunction expansion. Barrett and Squire (1996) extended the solution of Fox and Squire (1994) to two plates of arbitrary properties. Recently, the computational difficulties associated with the Wiener–Hopf solution of Evans and Davies (1968) have been overcome by Balmforth and Craster (1999), Chakrabarti (2000), Tkacheva (2001), and by Chung and Fox (2002). Chung and Linton (2005) have also solved the problem of open water and a semi-infinite plate using the residue calculus technique, a method which is closely related to the Wiener–Hopf method.

The closest solution to the one presented here was derived by Hermans (2004), based on an earlier solution for a single plate (Hermans, 2003). This solution was for a set of finite elastic plates of arbitrary properties. That problem differed from the one presented here, only by requiring that the semi-infinite regions are open water. The solution method presented in Hermans (2004) was quite different from the one presented here, and it was based on using the free-surface Green function.

We develop here a solution to the problem of wave propagation under many floating elastic plates of variable properties. We assume that the first and last plate are semi-infinite. Our solution allows us to consider the case of open water, by taking the limit as the plate thickness tends to zero. The solution is derived using an extended eigenfunction matching method, in which the plate boundary conditions are satisfied as auxiliary equations. We show that our solutions satisfy the energy balance condition, and that they agree with the results found by the method of Porter and Evans (2006). We also compare solutions with experiments which have recently been performed in a two-dimensional wave tank, using floating elastic plates of various geometries. These experiments, which were motivated by modelling wave propagation under floating ice sheets, are described in Sakai and Hanai (2002).

This work is the first step in a program to develop a model for wave propagation in the marginal ice zone. We require a solution for wave scattering which, while two-dimensional, is sufficiently flexible that it can include effects such as variable plate thickness and regions of open water. We require a high degree of confidence in the correctness of our numerical solution if it is to be used in a marginal ice zone model, and for this reason we focus on presenting results which establish the accuracy of the solution.

2. Formulation and preliminaries

We consider the problem of small-amplitude waves which are incident on a set of floating elastic plates occupying the entire water surface. The submergence of the plates is considered negligible. The extension of the method to submerged plates may be possible by modifying the present formulation but this remains a subject for future research. We assume that the problem is invariant in the y direction, although we allow the waves to be incident from an angle. The set of plates consists of two semi-infinite plates, separated by a region which consists of a finite number of plates with variable properties. We note that we can simulate open water by setting the plate properties, i.e. thickness, to be small or by introducing an additional formulation. To keep the presentation and the computer code which we have developed as simple as possible, we will not present an additional formulation, and we simply set the plate parameters to be sufficiently small if we require open water for any calculations. We also assume that the plate edges are free to move at each boundary, although other boundary conditions could easily be considered using the methods of solution presented here. A schematic diagram of the problem is shown in Fig. 1.

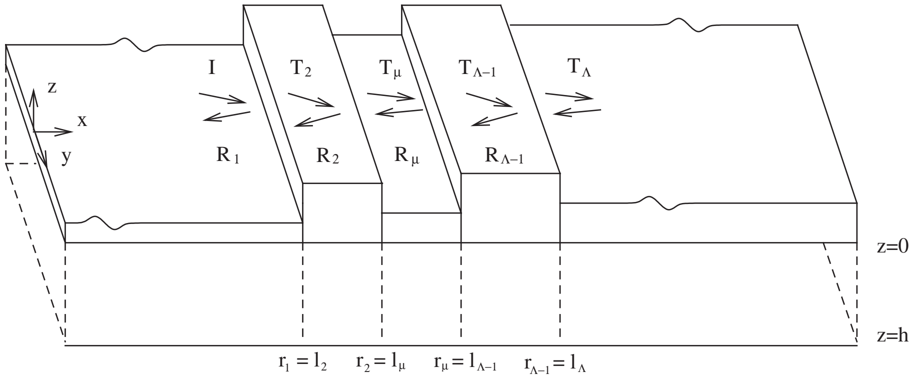

Fig. 1. A schematic diagram showing the set of floating elastic plates and the coordinate systems used in the solution. The three-dimensional region is defined by $-\infty < x, y < \infty$ and $-h < z \leqslant 0$. I represents the incident wave. R_μ and T_μ represent the reflection and transmission coefficients of the μth plate, l_μ and r_μ represent the left and right edge of the plate μ and Λ represents the last plate.

2.1. Assumptions and conditions

We assume that in the fluid region $-\infty < x, y < \infty$ and $-h < z \leqslant 0$, the flow is irrotational and inviscid, so that the fluid velocity can be written as the gradient of a velocity potential Φ which satisfies Laplace's equation in the fluid region, i.e.

$$\nabla^2 \Phi = 0 \quad \text{for } -h < z \leqslant 0. \tag{1}$$

We consider only incident waves of a single frequency ω, and we assume that these waves also have a simple harmonic variation with respect to y. The velocity potential of the wave can therefore be expressed as (Stoker, 1957; Fox and Squire, 1994):

$$\Phi(x, y, z, t) = \Re\{\phi(x, z)\, \mathrm{e}^{\mathrm{i}k_y y}\, \mathrm{e}^{-\mathrm{i}\omega t}\}, \tag{2}$$

where ϕ is the complex-valued potential, k_y is the wave number in the y direction and $\Re$ denotes the real part.

We assume that the seabed is impermeable, and therefore the velocity component normal to the sea floor vanishes. Hence, the velocity potential at the sea floor satisfies

$$\frac{\partial \Phi}{\partial z} = 0 \quad \text{at } z = -h. \tag{3}$$

The corresponding elevation of the plates is defined by $\Re\{\eta(x)\, \mathrm{e}^{\mathrm{i}k_y y}\, \mathrm{e}^{-\mathrm{i}\omega t}\}$ where, using the linear kinematic condition at the free surface

$$-\mathrm{i}\omega\eta = \frac{\partial \phi}{\partial z} \quad \text{at } z = 0 \tag{4}$$

(Billingham and King, 2000). We assume the μth elastic plate has mass density ρ_μ and thickness d_μ. We assume that the amplitude at the free surface is small relative to the wavelength and that the curvature is small and hence linearity can be applied. The equation of motion for the plate is therefore given by the elastic plate equation

$$P = D_\mu \left(\frac{\partial^2}{\partial x^2} - k_y^2 \right)^2 \eta - \omega^2 m_\mu \eta \quad \text{at } z = 0, \; l_\mu \leqslant x \leqslant r_\mu \tag{5}$$

(Wang and Meylan, 2004) where P is the pressure at the surface, D_μ is the rigidity constant of the μth plate and $m_\mu = \rho_\mu d_\mu$. The dynamic condition given by the linearised Bernoulli equation applies

$$-\mathrm{i}\omega\phi + \frac{P}{\rho} + g\eta = 0 \quad \text{at } z = 0 \tag{6}$$

(Stoker, 1957), where P is the pressure at the water surface and ρ is the water density. Equating Eqs. (5) and (6) gives

$$D_\mu \left(\frac{\partial^2}{\partial x^2} - k_y^2 \right)^2 \eta - \omega^2 m_\mu \eta - \mathrm{i}\omega\rho\phi + \rho g \eta = 0 \quad \text{at } z = 0, \; l_\mu \leqslant x \leqslant r_\mu. \tag{7}$$

Additional constraints apply at the edges of the elastic plates (Fox and Squire, 1994). We assume that the plate edges are free, which implies that the bending moment and the shearing forces at the edges are zero. Therefore, the edge boundary conditions can be expressed as

$$\left(\frac{\partial^3}{\partial x^3} - (2-v)k_y^2\frac{\partial}{\partial x}\right)\eta = 0 \quad \text{at } z=0 \text{ for } x = l_\mu, r_\mu, \tag{8}$$

$$\left(\frac{\partial^3}{\partial x^2} - vk_y^2\right)\eta = 0 \text{ for } \quad \text{at } z=0 \text{ for } x = l_\mu, r_\mu, \tag{9}$$

where v is Poisson's constant and l_μ and r_μ represent the left and right edge of the μth plate as shown in Fig. 1.

2.2. Nondimensionalising the variables

It is convenient to reduce the number of constants in the equations by nondimensionalising. We nondimensionalise by scaling the spatial variables by a length parameter L, and the time variables by a time parameter $\sqrt{L/g}$. We leave open the choice of length parameter L. The nondimensional variables, (denoted by an overbar) are

$$\bar{x} = \frac{x}{L}, \quad \bar{y} = \frac{y}{L}, \quad \bar{z} = \frac{z}{L}, \quad \bar{\eta} = \frac{\eta}{L}, \quad \bar{t} = \frac{t}{\sqrt{g/L}} \quad \text{and} \quad \bar{\phi} = \frac{\phi}{L\sqrt{Lg}}.$$

The boundary condition given by Eq. (7) can now be nondimensionally expressed as

$$\beta_\mu\left(\frac{\partial^2}{\partial \bar{x}^2} - \bar{k}_y^2\right)^2\bar{\eta} - \bar{\omega}^2\gamma_\mu\bar{\eta} - \mathrm{i}\bar{\omega}\bar{\phi} + \bar{\eta} = 0 \quad \text{at } z=0,\ \bar{l}_\mu \leqslant \bar{x} \leqslant \bar{r}_\mu, \tag{10}$$

where $\beta_\mu = D_\mu/\rho_\mu g L^4$ is referred to as the stiffness constant and $\gamma_\mu = m_\mu/\rho L$ is referred to as the mass constant. From here on in, all equations are expressed nondimensionally, and for simplicity the overbar will be omitted from the dimensionless variables in what follows.

2.3. Final equations

Eliminating η using Eq. (4), Eqs. (1), (3), (8), (9), and (10) become

$$\left(\frac{\partial^2}{\partial x^2} + \frac{\partial^2}{\partial z^2} - k_y^2\right)\phi = 0 \quad \text{for } -h < z \leqslant 0, \tag{11}$$

$$\frac{\partial\phi}{\partial z} = 0 \quad \text{at } z = -h, \tag{12}$$

$$\left(\beta_\mu\left(\frac{\partial^2}{\partial x^2} - k_y^2\right)^2 - \gamma_\mu\alpha + 1\right)\frac{\partial\phi}{\partial z} - \alpha\phi = 0 \quad \text{at } z=0,\ l_\mu \leqslant x \leqslant r_\mu, \tag{13}$$

where $\alpha = \omega^2$ and

$$\left(\frac{\partial^3}{\partial x^3} - (2-v)k_y^2\frac{\partial}{\partial x}\right)\frac{\partial\phi}{\partial z} = 0 \quad \text{at } z=0 \text{ for } x = l_\mu, r_\mu, \tag{14}$$

$$\left(\frac{\partial^2}{\partial x^2} - vk_y^2\right)\frac{\partial\phi}{\partial z} = 0 \text{ for } \quad \text{at } z=0 \text{ for } x = l_\mu, r_\mu. \tag{15}$$

3. Method of solution

3.1. Eigenfunction expansion

We shall solve Eqs. (11)–(15) using an eigenfunction expansion. This method has been applied in many situations for linear water wave problems, and the technique is described in Linton and McIver (2001). The method was developed by Fox and Squire (1994) for the case of the elastic plate boundary condition, and subsequently it has been used by Barrett and Squire (1996), Sahoo et al. (2001) and Teng et al. (2001). We show here how this method can be extended to the case of an arbitrary number of plates. One of the key features in the eigenfunction expansion method for elastic plates is that extra modes are required in order to solve the higher order boundary conditions at the plate edges. The first and last plates are semi-infinite and the middle plates are finite. The potential velocity of the first plate can be expressed as the summation of an incident wave and of reflected waves, one of which is propagating but the rest are evanescent and they decay as x tends to $-\infty$. Similarly the potential under the final plate can be expressed as a sum of transmitting waves, one of which is propagating and the rest are evanescent and decay towards $+\infty$. The potential under the middle plates can be expressed as the sum of transmitting waves and reflected waves, each of which consists of a propagating wave plus evanescent waves which decay as x decreases or increases, respectively. We could combine these waves in the formulation, but because of the exponential growth (or decay) in the x direction the solution becomes numerically unstable in some cases if the transmission and reflection are not expanded at opposite ends of the plate.

3.2. Separation of variables

The potential velocity can be written in terms of an infinite series of separated eigenfunctions under each elastic plate, of the form

$$\phi = \mathrm{e}^{\kappa_\mu x}\cos(k_\mu(z+h)).$$

If we apply the boundary conditions given by Eqs. (12) and (13) we obtain

$$k_\mu \tan(k_\mu h) = -\frac{\alpha}{\beta_\mu k_\mu^4 + 1 - \alpha\gamma_\mu} \tag{16}$$

(Fox and Squire, 1994). Solving for k_μ, this dispersion Eq. (16) gives a pure imaginary root with positive imaginary part, two complex roots (two complex conjugate paired roots with positive imaginary part in all physical situations), an infinite number of positive real roots which approach $n\pi/h$ as n approaches infinity, and also the negative of all these roots (Fox and Squire, 1994). We denote the two complex roots with positive imaginary part by $k_\mu(-2)$ and $k_\mu(-1)$, the purely imaginary root with positive imaginary part by $k_\mu(0)$ and the real roots with positive imaginary part by $k_\mu(n)$ for n a positive integer. The imaginary root with positive imaginary part corresponds to a reflected travelling mode propagating along the x axis. The complex roots with positive imaginary parts correspond to damped reflected travelling modes and the real roots correspond to reflected evanescent modes. In a similar manner, the negative of these correspond to the transmitted travelling, damped and evanescent modes, respectively. The coefficient κ_μ is

$$\kappa_\mu(n) = \sqrt{k_\mu(n)^2 + k_y^2},$$

where the root with positive real part is chosen or if the real part is negative with negative imaginary part. Note that the solutions of the dispersion equation will be different under plates of different properties, and that the expansion is only valid under a single plate. We will solve for the coefficients in the expansion by matching the potential and its x derivative at each boundary and by applying the boundary conditions at the edge of each plate.

3.3. Expressions for the potential velocity

We now expand the potential under each plate using the separation of variables solution. We always include the two complex and one imaginary root, and truncate the expansion at M real roots of the dispersion equation. The potential ϕ can now be expressed as the following sum of eigenfunctions:

$$\phi \approx \begin{cases} I\mathrm{e}^{\kappa_1(0)(x-r_1)}\dfrac{\cos(k_1(0)(z+h))}{\cos(k_1(0)h)} + \displaystyle\sum_{n=-2}^{M} R_1(n)\,\mathrm{e}^{\kappa_1(n)(x-r_1)}\dfrac{\cos(k_1(n)(z+h))}{\cos(k_1(n)h)} & \text{for } x<r_1, \\ \displaystyle\sum_{n=-2}^{M} T_\mu(n)\mathrm{e}^{-\kappa_\mu(n)(x-l_\mu)}\dfrac{\cos(k_\mu(n)(z+h))}{\cos(k_\mu(n)h)} + \displaystyle\sum_{n=-2}^{M} R_\mu(n)\,\mathrm{e}^{\kappa_\mu(n)(x-r_\mu)}\dfrac{\cos(k_\mu(n)(z+h))}{\cos(k_\mu(n)h)} & \text{for } l_\mu<x<r_\mu, \\ \displaystyle\sum_{n=-2}^{M} T_\Lambda(n)\mathrm{e}^{-\kappa_\Lambda(n)(x-l_\Lambda)}\dfrac{\cos(k_\Lambda(n)(z+h))}{\cos(k_\Lambda(n)h)} & \text{for } l_\Lambda<x, \end{cases} \tag{17}$$

where I is the nondimensional incident wave amplitude in potential, μ is the μth plate, Λ is the last plate, r_μ represents the x-coordinate of the right edge of the μth plate, $l_\mu(=r_{\mu-1})$ represents the x-coordinate of the left edge of the μth plate, $R_\mu(n)$ represents the reflected potential coefficient of the nth mode under the μth plate, and $T_\mu(n)$ represents the transmitted potential coefficient of the nth mode under the μth plate. Note that we have divided by $\cos(kh)$, so that the coefficients are normalised by the potential at the free surface rather than at the bottom surface.

3.4. Expressions for displacement

The displacement is given by

$$\eta \approx \frac{\mathrm{i}}{\omega}\begin{cases} Ik_1(0)\mathrm{e}^{\kappa_1(0)(x-r_1)}\tan(k_1(0)h) - \sum\limits_{n=-2}^{M} R_1(n)k_1(n)\,\mathrm{e}^{\kappa_1(n)(x-r_1)}\tan(k_1(n)h) & \text{for } x<r_1, \\ -\sum\limits_{n=-2}^{M} T_\mu(n)k_\mu(n)\mathrm{e}^{-\kappa_\mu(n)(x-l_\mu)}\tan(k_\mu(n)h) & \\ -\sum\limits_{n=-2}^{M} R_\mu(n)k_\mu(n)\,\mathrm{e}^{\kappa_\mu(n)(x-r_\mu)}\tan(k_\mu(n)h) & \text{for } l_\mu<x<r_\mu, \\ -\sum\limits_{n=-2}^{M} T_\Lambda(n)k_\mu(n)\mathrm{e}^{-\kappa_\mu(n)(x-l_\Lambda)}\tan(k_\mu(n)h) & \text{for } l_\Lambda<x. \end{cases} \tag{18}$$

3.5. Solving via eigenfunction matching

To solve for the coefficients, we require as many equations as we have unknowns. We derive the equations from the free edge conditions and from imposing conditions of continuity of the potential and its derivative in the x-direction at each plate boundary. We impose the latter condition by taking inner products with respect to the orthogonal functions $\cos((m\pi/h)(z+h))$, where m is a natural number. These functions are chosen for the following reasons. The vertical eigenfunctions $\cos(k_\mu(n)(z+h))$ are not orthogonal (they are not even a basis) and could therefore lead to an ill-conditioned system of equations. Furthermore, by choosing $\cos((m\pi/h)(z+h))$ we can use the same functions to take the inner products under every plate. Finally, and most importantly, the plate eigenfunctions approach $\cos((m\pi/h)(z+h))$ for large m, so that as we increase the number of modes the matrices become almost diagonal, leading to a very well-conditioned system of equations.

Taking inner products leads to the following equations

$$\int_{-h}^{0}\phi_\mu(r_\mu,z)\cos\left(\frac{m\pi}{h}(z+h)\right)\mathrm{d}z = \int_{-h}^{0}\phi_{\mu+1}(l_{\mu+1},z)\cos\left(\frac{m\pi}{h}(z+h)\right)\mathrm{d}z,$$

$$\int_{-h}^{0}\frac{\partial\phi_\mu}{\partial x}(r_\mu,z)\cos\left(\frac{m\pi}{h}(z+h)\right)\mathrm{d}z = \int_{-h}^{0}\frac{\partial\phi_{\mu+1}}{\partial x}(l_{\mu+1},z)\cos\left(\frac{m\pi}{h}(z+h)\right)\mathrm{d}z, \tag{19}$$

where $m\in[0,M]$ and ϕ_μ denotes the potential under the μth plate, i.e. the expression for ϕ given by Eq. (17) valid for $l_\mu<x<r_\mu$. The remaining equations to be solved are given by the two edge conditions satisfied at both edges of each plate

$$\left(\frac{\partial^3}{\partial x^3} - (2-\nu)k_y^2\frac{\partial}{\partial x}\right)\frac{\partial\phi_\mu}{\partial z} = 0 \quad \text{for } z=0 \text{ and } x=l_\mu, r_\mu,$$

$$\left(\frac{\partial^2}{\partial x^2} - \nu k_y^2\right)\frac{\partial\phi_\mu}{\partial z} = 0 \quad \text{for } z=0 \text{ and } x=l_\mu, r_\mu. \tag{20}$$

We shall show the explicit form of the linear system of equations which arise when we solve Eqs. (19) and (20). Let $\mathbf{T}_\mu$ be a column vector given by $[T_\mu(-2),\ldots,T_\mu(M)]^{\mathrm{T}}$ and $\mathbf{R}_\mu$ be a column vector given by $[R_\mu(-2)\ldots R_\mu(M)]^{\mathrm{T}}$.

The equations which arise from matching at the boundary between the first and second plate are

$$I\mathbf{C} + \mathbf{M}^+_{R_1}\mathbf{R}_1 = \mathbf{M}^-_{T_2}\mathbf{T}_2 + \mathbf{M}^-_{R_2}\mathbf{R}_2, \quad -\kappa_1(0)I\mathbf{C} + \mathbf{N}^+_{R_1}\mathbf{R}_1 = \mathbf{N}^-_{T_2}\mathbf{T}_2 + \mathbf{N}^-_{R_2}\mathbf{R}_2. \tag{21}$$

The equations which arise from matching at the boundary of the μth and $(\mu+1)$th plate boundary $(\mu>1)$ are

$$\mathbf{M}^+_{T_\mu}\mathbf{T}_\mu + \mathbf{M}^+_{R_\mu}\mathbf{R}_\mu = \mathbf{M}^-_{T_{\mu+1}}\mathbf{T}_{\mu+1} + \mathbf{M}^-_{R_{\mu+1}}\mathbf{R}_{\mu+1}, \quad \mathbf{N}^+_{T_\mu}\mathbf{T}_\mu + \mathbf{N}^+_{R_\mu}\mathbf{R}_\mu = \mathbf{N}^-_{T_{\mu+1}}\mathbf{T}_{\mu+1} + \mathbf{N}^-_{R_{\mu+1}}\mathbf{R}_{\mu+1}. \tag{22}$$

The equations which arise from matching at the $(\Lambda-1)$th and Λth boundary are

$$\mathbf{M}^+_{T_{\Lambda-1}}\mathbf{T}_{\Lambda-1} + \mathbf{M}^+_{R_{\Lambda-1}}\mathbf{R}_{\Lambda-1} = \mathbf{M}^-_{T_\Lambda}\mathbf{T}_\Lambda, \quad \mathbf{N}^+_{T_{\Lambda-1}}\mathbf{T}_{\Lambda-1} + \mathbf{N}^+_{R_{\Lambda-1}}\mathbf{R}_{\Lambda-1} = \mathbf{N}^-_{T_\Lambda}\mathbf{T}_\Lambda, \tag{23}$$

where $\mathbf{M}^+_{T_\mu}, \mathbf{M}^+_{R_\mu}, \mathbf{M}^-_{T_\mu}$, and $\mathbf{M}^-_{R_\mu}$ are $(M+1)$ by $(M+3)$ matrices given by

$$\mathbf{M}^+_{T_\mu}(m,n) = \int_{-h}^{0} \mathrm{e}^{-\kappa_\mu(n)(r_\mu - l_\mu)} \frac{\cos(k_\mu(n)(z+h))}{\cos(k_\mu(n)h)} \cos\left(\frac{m\pi}{h}(z+h)\right) \mathrm{d}z,$$
$$\mathbf{M}^+_{R_\mu}(m,n) = \int_{-h}^{0} \frac{\cos(k_\mu(n)(z+h))}{\cos(k_\mu(n)h)} \cos\left(\frac{m\pi}{h}(z+h)\right) \mathrm{d}z, \tag{24}$$

$$\mathbf{M}^-_{T_\mu}(m,n) = \mathbf{M}^+_{R_\mu}(m,n), \quad \mathbf{M}^-_{R_\mu}(m,n) = \mathbf{M}^+_{T_\mu}(m,n).$$

$\mathbf{N}^+_{T_\mu}, \mathbf{N}^+_{R_\mu}, \mathbf{N}^-_{T_\mu}$, and $\mathbf{N}^-_{R_\mu}$ are given by

$$\mathbf{N}^\pm_{T_\mu}(m,n) = -\kappa_\mu(n)\mathbf{M}^\pm_{T_\mu}(m,n), \quad \mathbf{N}^\pm_{R_\mu}(m,n) = \kappa_\mu(n)\mathbf{M}^\pm_{R_\mu}(m,n). \tag{25}$$

$\mathbf{C}$ is a $(M+1)$ vector which is given by

$$\mathbf{C}(m) = \int_{-h}^{0} \frac{\cos(k_1(0)(z+h))}{\cos(k_1(0)h)} \cos\left(\frac{m\pi}{h}(z+h)\right) \mathrm{d}z. \tag{26}$$

The integrals in Eqs. (24) and (26) are each solved analytically. Now, for all but the first and Λth plate, Eq. (20) becomes

$$\mathbf{E}^+_{T_\mu}\mathbf{T}_\mu + \mathbf{E}^+_{R_\mu}\mathbf{R}_\mu = \mathbf{0}, \quad \mathbf{E}^-_{T_\mu}\mathbf{T}_\mu + \mathbf{E}^-_{R_\mu}\mathbf{R}_\mu = \mathbf{0}. \tag{27}$$

The first and last plates only require two equations, because each has only one plate edge. The equation for the first plate must be modified to include the effect of the incident wave. This gives us

$$I\begin{pmatrix} \mathbf{E}^+_{T_1}(1,0) \\ \mathbf{E}^+_{T_1}(2,0) \end{pmatrix} + \mathbf{E}^+_{R_1}\mathbf{R}_1 = \mathbf{0}, \tag{28}$$

and for the Λth plate we have no reflection so

$$\mathbf{E}^-_{T_\mu}\mathbf{T}_\mu = \mathbf{0}. \tag{29}$$

$\mathbf{E}^+_{T_\mu}, \mathbf{E}^+_{R_\mu}, \mathbf{E}^-_{T_\mu}$ and $\mathbf{E}^-_{R_\mu}$ are $2 \times (M+1)$ matrices given by

$$\mathbf{E}^-_{T_\mu}(1,n) = (\kappa_\mu(n)^2 - (2-v)k_y^2)(k_\mu(n)\kappa_\mu(n)\tan(k_\mu(n)h)),$$
$$\mathbf{E}^+_{T_\mu}(1,n) = (\kappa_\mu(n)^2 - (2-v)k_y^2)(k_\mu(n)\kappa_\mu(n)\,\mathrm{e}^{-\kappa_\mu(n)(r_\mu - l_\mu)}\tan(k_\mu(n)h)),$$
$$\mathbf{E}^-_{R_\mu}(1,n) = (\kappa_\mu(n)^2 - (2-v)k_y^2)(-k_\mu(n)\kappa_\mu(n)\,\mathrm{e}^{\kappa_\mu(n)(l_\mu - r_\mu)}\tan(k_\mu(n)h)),$$
$$\mathbf{E}^+_{R_\mu}(1,n) = (\kappa_\mu(n)^2 - (2-v)k_y^2)(-k_\mu(n)\kappa_\mu(n)\tan(k_\mu(n)h)),$$
$$\mathbf{E}^-_{T_\mu}(2,n) = (\kappa_\mu(n)^2 - vk_y^2)(-k_\mu(n)\tan(k_\mu(n)h)),$$
$$\mathbf{E}^+_{T_\mu}(2,n) = (\kappa_\mu(n)^2 - vk_y^2)(-k_\mu(n)\,\mathrm{e}^{-\kappa_\mu(n)(r_\mu - l_\mu)}\tan(k_\mu(n)h)),$$
$$\mathbf{E}^-_{R_\mu}(2,n) = (\kappa_\mu(n)^2 - vk_y^2)(-k_\mu(n)\,\mathrm{e}^{\kappa_\mu(n)(l_\mu - r_\mu)}\tan(k_\mu(n)h)),$$
$$\mathbf{E}^+_{R_\mu}(2,n) = (\kappa_\mu(n)^2 - vk_y^2)(-k_\mu(n)\tan(k_\mu(n)h)). \tag{30}$$

Now, the matching matrix is a $(2M+6) \times (\Lambda - 1)$ by $(2M+1) \times (\Lambda - 1)$ matrix given by

$$\mathbf{M} = \begin{pmatrix} \mathbf{M}^+_{R_1} & -\mathbf{M}^-_{T_2} & -\mathbf{M}^-_{R_2} & 0 & 0 & & 0 & 0 & 0 \\ \mathbf{N}^+_{R_1} & -\mathbf{N}^-_{T_2} & -\mathbf{N}^-_{R_2} & 0 & 0 & & 0 & 0 & 0 \\ 0 & \mathbf{M}^+_{T_2} & \mathbf{M}^+_{R_2} & -\mathbf{M}^-_{T_3} & -\mathbf{M}^-_{R_3} & \cdots & 0 & 0 & 0 \\ 0 & \mathbf{N}^+_{T_2} & \mathbf{N}^+_{R_2} & -\mathbf{N}^-_{T_3} & -\mathbf{N}^-_{R_3} & & 0 & 0 & 0 \\ & & \vdots & & & \ddots & & & \\ 0 & 0 & 0 & 0 & 0 & & \mathbf{M}^+_{T_{\Lambda-1}} & \mathbf{M}^+_{R_{\Lambda-1}} & -\mathbf{M}^-_{T_\Lambda} \\ 0 & 0 & 0 & 0 & 0 & & \mathbf{N}^+_{T_{\Lambda-1}} & \mathbf{N}^+_{R_{\Lambda-1}} & -\mathbf{N}^-_{T_\Lambda} \end{pmatrix}; \tag{31}$$

the edge matrix is a $(2M+6)\times(\Lambda-1)$ by $4(\Lambda-1)$ matrix given by

$$\mathbf{E} = \begin{pmatrix} \mathbf{E}^+_{R_1} & 0 & 0 & 0 & 0 & & 0 & 0 & 0 \\ 0 & \mathbf{E}^+_{T_2} & \mathbf{E}^+_{R_2} & 0 & 0 & & 0 & 0 & 0 \\ 0 & \mathbf{E}^-_{T_2} & \mathbf{E}^-_{R_2} & 0 & 0 & & 0 & 0 & 0 \\ 0 & 0 & 0 & \mathbf{E}^+_{T_3} & \mathbf{E}^+_{R_3} & \cdots & 0 & 0 & 0 \\ 0 & 0 & 0 & \mathbf{E}^-_{T_3} & \mathbf{E}^-_{R_3} & & 0 & 0 & 0 \\ & & \vdots & & & \ddots & & & \\ 0 & 0 & 0 & 0 & 0 & & \mathbf{E}^+_{T_{\Lambda-1}} & \mathbf{E}^+_{R_{\Lambda-1}} & 0 \\ 0 & 0 & 0 & 0 & 0 & & \mathbf{E}^-_{T_{\Lambda-1}} & \mathbf{E}^-_{R_{\Lambda-1}} & 0 \\ 0 & 0 & 0 & 0 & 0 & & 0 & 0 & \mathbf{E}^-_{T_\Lambda} \end{pmatrix}; \tag{32}$$

and finally the complete system to be solved is given by

$$\begin{pmatrix} \mathbf{M} \\ \mathbf{E} \end{pmatrix} \times \begin{pmatrix} \mathbf{R}_1 \\ \mathbf{T}_2 \\ \mathbf{R}_2 \\ \mathbf{T}_3 \\ \mathbf{R}_3 \\ \vdots \\ \mathbf{T}_{\Lambda-1} \\ \mathbf{R}_{\Lambda-1} \\ \mathbf{T}_\Lambda \end{pmatrix} = \begin{pmatrix} -I\mathbf{C} \\ \kappa_1(0) I\mathbf{C} \\ 0 \\ \vdots \\ -IE^+_{T_1}(1,0) \\ -IE^+_{T_1}(2,0) \\ 0 \\ \vdots \end{pmatrix}. \tag{33}$$

The final system of equations has size $(2M+6)\times(\Lambda-1)$ by $(2M+6)\times(\Lambda-1)$. The method of solution we have derived is relatively simple and leads to large systems of equations when we simulate multiple plates. Our aim is to produce code which is simple to develop and in which we have a strong degree of confidence, and one that is numerically accurate and error free. We do not want to make any kind of wide-spacing approximations since real ice fields always have some small floes which we want to be able to simulate. We have used our method to solve for up to a 100 plates in simulations of wave propagation in the marginal ice zone.

The system of equations has a large number of zero entries, due to the fact that each plate couples only with its nearest neighbour. It seems likely that a more sophisticated method of solution could be developed, which exploits this structure. We have been unable to find such a method due to the difficulty of including the free edge conditions.

4. Validation of the solutions

4.1. Energy balance

An energy balance relation is derived in Evans and Davies (1968) which is simply a condition that the incident energy is equal to the sum of the radiated energy including both the energy in the water and the energy in the plate. If the properties of the first and last semi-infinite plates were identical, then this would be the familiar requirement that

$$|T_\Lambda(0)|^2 + |R_1(0)|^2 = |I|^2.$$

However, when the first and last plates have different properties, then the energy balance condition becomes the following:

$$D|T_\Lambda(0)|^2 + |R_1(0)|^2 = |I|^2, \tag{34}$$

where D is found by applying Green's theorem to ϕ and its conjugate (Evans and Davies, 1968) and is given by

$$D = \frac{\kappa_A(0)k_1(0)\cosh^2(k_1(0)h)}{\kappa_1(0)k_A(0)\cosh^2(k_A(0)h)} \times \frac{\left(\frac{\beta_A}{\alpha}4k_A(0)^3(\kappa_A(0)^2+k_y^2)\sinh^2(k_A(0)h)+\frac{1}{2}\sinh(2k_A(0)h)+k_A(0)h\right)}{\left(\frac{\beta_1}{\alpha}4k_1(0)^3(\kappa_1(0)^2+k_y^2)\sinh^2(k_1(0)h)+\frac{1}{2}\sinh(2k_1(0)h)+k_1(0)h\right)}. \tag{35}$$

The energy balance condition is useful to help check that the solution is not incorrect (it does not of course guarantee that the solution is correct). The energy balance condition is surprisingly well satisfied by our solutions, for example with $M = 20$ we can easily get 10 decimal places.

4.2. Oblique waves through a set of elastic plates with uniform properties

The solution method we present can be used to solve many of the simpler problems which have been considered in previous works. For example, we can solve for the problem of a single plate surrounded by water, or for a crack between two semi-infinite plates. We choose here to compare our results with the results of Porter and Evans (2006), who solved for the reflection and transmission of flexural-gravity waves propagating obliquely through a set of elastic plates separated by narrow parallel cracks. This is equivalent to our problem if the properties are identical for each elastic plate (the plates are of constant thickness, Young's modulus etc.). We have selected this solution to compare with, because the most challenging aspect of our problem is the fact that we have multiple cracks. We have also compared our solution with a single plate surrounded by water and for the problem of a single crack between two plates. However, we do not present these comparisons here.

The solution of Porter and Evans (2006) expresses the potential ϕ in terms of a linear combination of the incident wave and certain source functions located at each of the cracks. Along with satisfying the field and boundary conditions, these source functions satisfy the jump conditions in the displacements and gradients across each crack.

We shall briefly present the solution of Porter and Evans (2006) in our notation and nondimensionalisation. Porter and Evans (2006) first define a function $\chi(x,z)$ representing outgoing waves as $|x| \to \infty$ which satisfies

$$(\nabla^2 - k_y^2)\chi = 0, \quad -h < z < 0, \quad -\infty < x < \infty, \tag{36}$$

$$\frac{\partial \chi}{\partial z} = 0, \quad z = -h, \quad -\infty < x < \infty, \tag{37}$$

$$\left(\beta\left(\frac{\partial^2}{\partial x^2} - k_y^2\right)^2 - \gamma\alpha + 1\right)\frac{\partial \chi}{\partial z} - \alpha\chi = \delta(x), \quad z = 0, \quad -\infty < x < \infty. \tag{38}$$

This problem can be solved to give

$$\chi(x,z) = -\mathrm{i}\sum_{n=-2}^{M}\frac{\sin(k(n)h)\cos(k(n)(z-h))}{2\alpha C_n}\mathrm{e}^{-\kappa(n)|x|}, \tag{39}$$

where

$$C_n = \frac{1}{2}\left(h + \frac{(5\beta k(n)^4 + 1 - \alpha\gamma)\sin^2(k(n)h)}{\alpha}\right), \tag{40}$$

and $k(n)$ are the solutions of the dispersion Eq. (16) (remembering that the plate properties are all identical, so that there is only a single dispersion equation to solve and we have removed the μ subscript).

Consequently, the source functions for a single crack at $x = 0$ can be defined as

$$\psi_s(x,z) = \beta(\chi_{xx}(x,z) - vk_y^2\chi(x,z)), \quad \psi_a(x,z) = \beta(\chi_{xxx}(x,z) - v_1k_y^2\chi_x(x,z)), \tag{41}$$

where $v_1 = 2 - v$. It can easily be shown that ψ_s is symmetric about $x = 0$ and ψ_a is antisymmetric about $x = 0$.

Substituting Eq. (39) into Eq. (41) gives

$$\psi_s(x,z) = -\frac{\beta}{\alpha}\sum_{n=-2}^{\infty}\frac{g_n\cos(k(n)(z+h))}{2k_{xn}C_n}\mathrm{e}^{\kappa_n|x|}, \quad \psi_a(x,z) = \mathrm{sgn}(x)\mathrm{i}\frac{\beta}{\alpha}\sum_{n=-2}^{\infty}\frac{g_n'\cos(k(n)(z+h))}{2k_{xn}C_n}\mathrm{e}^{\kappa_n|x|}, \tag{42}$$

where

$$g_n = -\mathrm{i}\kappa(n)(-\kappa(n)^2 + \nu k_y^2)(\sin(k(n)h)), \quad g'_n = \kappa(n)^2(-\kappa(n)^2 + \nu k_y^2)(\sin(k(n)h)).$$

Porter and Evans (2006) then express the solution to the problem as a linear combination of the incident wave and pairs of source functions at each crack,

$$\phi(x,z) = I\mathrm{e}^{-\kappa_1(0)(x-r_1)}\frac{\cos(k_1(0)(z+h))}{\cos(k_1(0)h)} + \sum_{n=1}^{\Lambda-1}(P_n\psi_s(x-r_n,z) + Q_n\psi_a(x-r_n,z)), \tag{43}$$

where P_n and Q_n are coefficients to be solved which represent the jump in the gradient and elevation, respectively, of the plates across the crack $x = a_j$. The coefficients P_n and Q_n are found by applying the edge conditions Eqs. (14) and (15) to the z derivative of ϕ at $z = 0$.

The reflection and transmission coefficients, $R_1(0)$ and $T_\Lambda(0)$ can be found from Eq. (43) by taking the limits as $x \to \pm\infty$ to obtain

$$R_1(0)\mathrm{e}^{-\kappa(0)r_1} = -\frac{\beta}{\alpha}\sum_{n=1}^{\Lambda-1}\frac{\mathrm{e}^{\kappa(0)r_n}}{2k_0C_0}(g'_0Q_n + \mathrm{i}g_0P_j), \quad T_\Lambda(0)\mathrm{e}^{\kappa(0)l_\Lambda} = 1 + \frac{\beta}{\alpha}\sum_{n=1}^{\Lambda-1}\frac{\mathrm{e}^{-\kappa(0)r_n}}{2k_0C_0}(g'_0Q_n - \mathrm{i}g_0P_j). \tag{44}$$

Fig. 2 shows a comparison between our results and results calculated using the theory of Porter and Evans (2006) for $\Lambda = 2$ and 4 with $\beta = 0.1$, $\gamma = 0$ and $h = 1$. The pluses and circles are the results using our theory, and the solid lines are due to Porter and Evans (2006). As can be seen from the figure, the two methods are in close agreement.

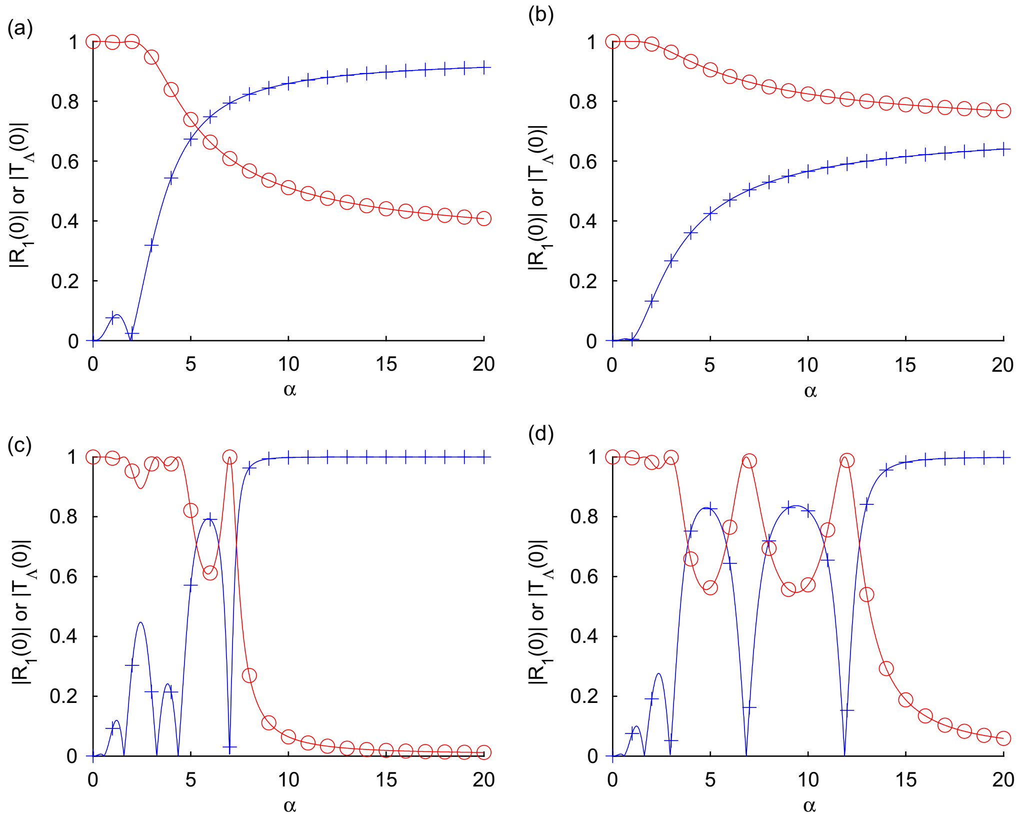

Fig. 2. $|R_1(0)|$ (pluses) and $|T_\Lambda(0)|$ (circles) versus α; $\beta = 0.1$, $\gamma = 0$ and $h = 1$: (a) solutions for two plates with the crack at $x = 0$ and with $\theta = 0$; (b) solutions for two plates with the crack at $x = 0$ and with $\theta = \pi/3$; (c) solutions for four plates with the cracks at $x = 0, 1, 2$ and with $\theta = 0$; (d) solutions for four plates with the cracks at $x = 0, 1, 2$ and with $\theta = \pi/12$.

Table 1
$|T|$ for $\alpha = 5$, $\beta = 0.1$, $\gamma = 0$, $h = 1$ and the values of Λ and M are shown, calculated by the present method and by the method in Porter and Evans (2006)

Λ	M	$\lvert T\rvert$ (present method)	$\lvert T\rvert$ (Porter and Evans, 2006)
2	5	0.72897005265395	0.68013661602795
	10	0.73710075717437	0.73382189306476
	20	0.73943613533854	0.73910099180859
	50	0.74014223492682	0.74012279625910
	100	0.74024743508561	0.74024507931561
	150	0.74026720286310	0.74026651629366
4	5	0.78572228609681	0.64049634405062
	10	0.81444198211422	0.80423931535963
	20	0.82228249776276	0.82126508433661
	50	0.82458694969417	0.82452862088603
	100	0.82492540871298	0.82491836384358
	150	0.82498871994750	0.82498666973497

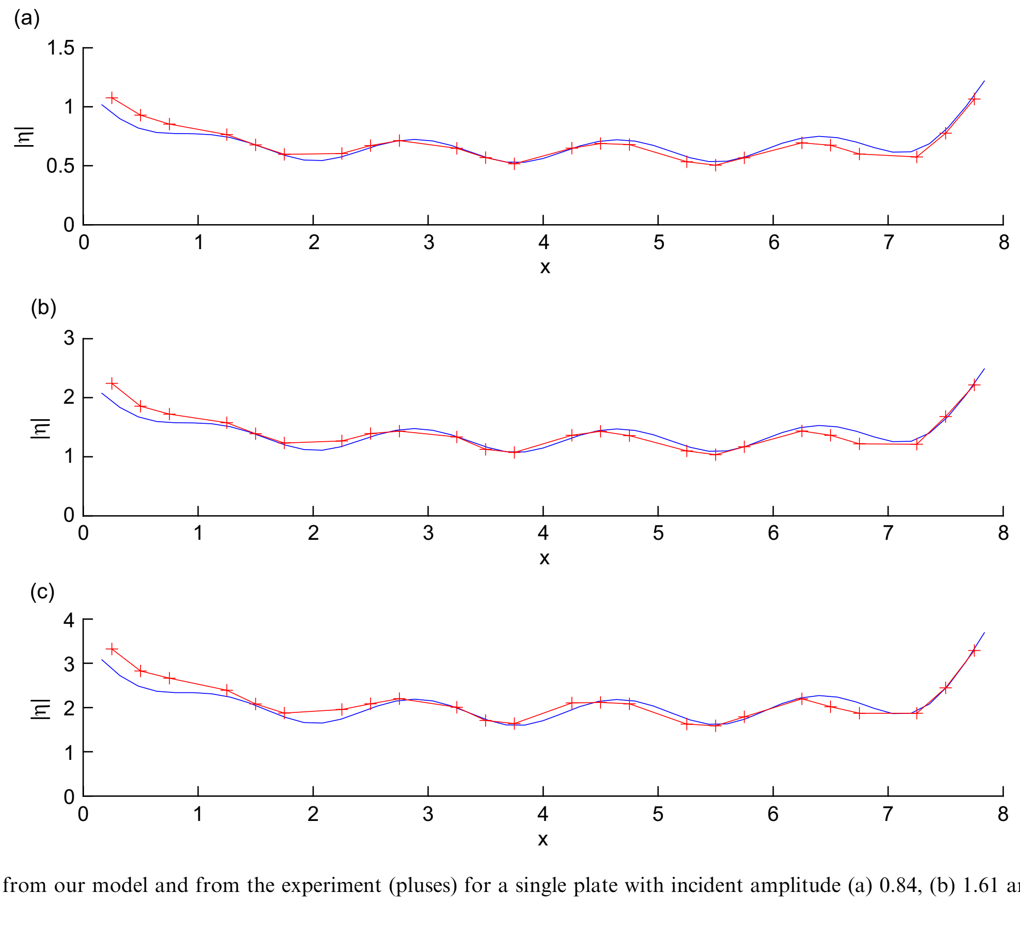

Fig. 3. $|\eta|$ from our model and from the experiment (pluses) for a single plate with incident amplitude (a) 0.84, (b) 1.61 and (c) 2.47 $T = 1.4\,\mathrm{s}$.

4.3. Solution convergence

We can use the solution of Porter and Evans (2006) to investigate the convergence of our solution. Table 1 shows $|T|$ for our method and for Porter and Evans (2006) as a function of M for $\Lambda = 2$ and 4, $\alpha = 5$, $\beta = 0.1$, $\gamma = 0$ and $h = 1$. The rate of convergence of the two solutions is almost identical. The accuracy of two decimal places for $M = 20$ is sufficient for most practical calculations.

4.4. Wave tank experiment

The solution method is also validated by comparison to a series of experiments which were performed in a two-dimensional wave tank. These experiments were aimed at simulating wave propagation in the marginal ice zone, and results concerned with determining the dispersion equation are described in Sakai and Hanai (2002). The wave tank used for the experiment was 26 m long, 0.8 m wide and 0.6 m deep. The waves were generated using a wave-maker set-up at the front of the tank, and an active wave absorption system was used at the far end of the tank. Elastic sheets were placed on the surface of the wave tank, with negligible gap. The plates occupied a length of 8 m of the tank and the entire width of the tank. We shall compare with the experiments which were performed with one 8 m sheet, two 4 m sheets and four 2 m sheets. The elastic plate was 20 mm thick, Young's modulus E was approximately 650 MPa and the density of the plate was 914 kg m^{-3}. The vertical displacement was measured at 25 different points along the plate using ultrasonic sensors. We assume that Poisson's ratio $\nu = 0.3$, $g = 9.8\,\mathrm{m\,s^{-2}}$ and the density of water $\rho = 1000\,\mathrm{kg\,m^{-3}}$.

Fig. 3 shows the results for a single plate with period $T = 1.4$ s for three different amplitudes. The figure plots the absolute value of the displacement as predicted by theory (solid line) with the results measured experimentally (pluses). As well as showing good agreement between measurement and theory, this figure also shows that the experimental

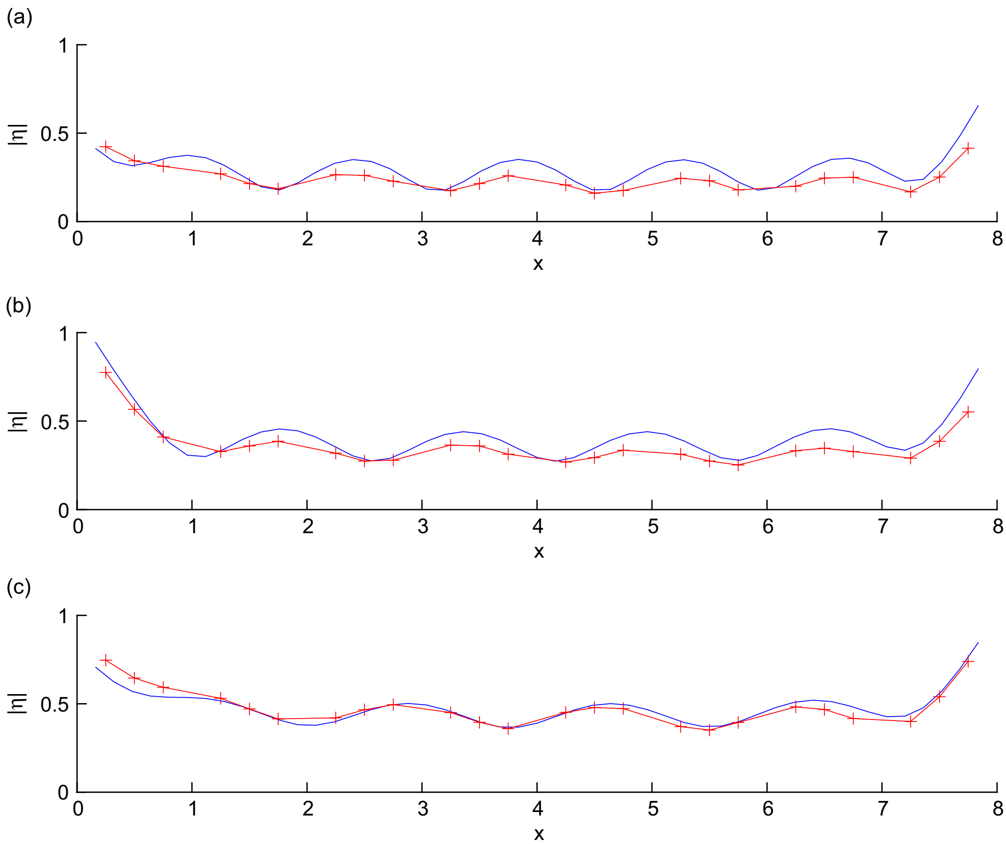

Fig. 4. $|\eta|$ from our model and from experiment (pluses) for a single plate for the wave periods (a) 1 s, (b) 1.2 s and (c) 1.4 s.

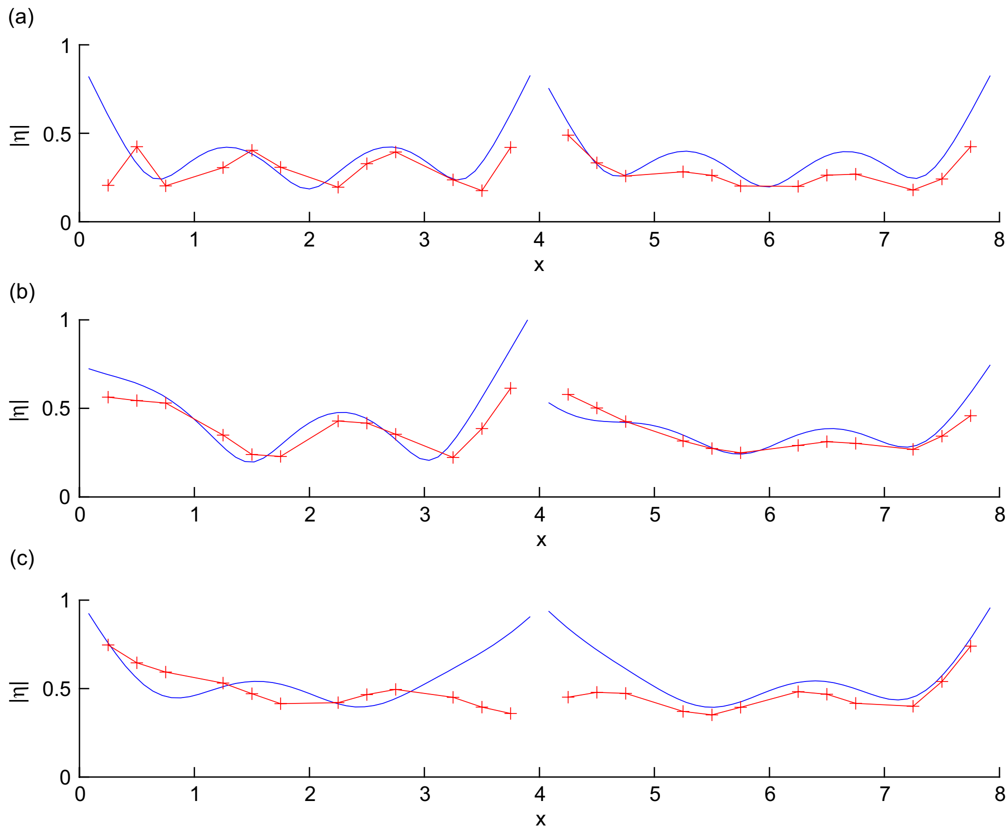

Fig. 5. As Fig. 4 except for two plates.

amplitudes are within the linear regime because there is little change in the measured results as the amplitude increases (apart from the uniform linear change).

Figs. 4–6 show the results for $T = 1$, 1.2 and 1.4 s for one, two and three plates, respectively. The figures show good agreement, with a trend of increasing agreement as the period increased. The only figure where there is poor agreement is Fig. 5 for 1.4 s. We are uncertain about the origin of this difference. However, the overall agreement is good, especially considering that we are plotting the amplitude of displacement. We consider this to be strong confirmation that our model is performing adequately. The cusps apparent in Fig. 6 for $T = 1$ s, are caused by the plates being so short as to be almost rigid and by having a near-zero in displacement. The effect, when plotting the absolute value of displacement, is a cusp.

5. Conclusions

We have solved for the linear water wave propagation under a set of floating elastic plates. While the problem was two-dimensional, it does allow the waves to be incident at an angle. The elastic plate properties can be set arbitrarily, so that the model can also include regions of open water. The solution method is based on an eigenfunction matching at the boundaries of the plates. We also impose the free-edge conditions at the plate edges, by deriving fewer equations from matching than there are unknowns. This is done in a very natural way because the eigenfunctions under the plate actually contain extra modes. The method is stable, but computationally demanding for a large number of plates.

We have compared our solution with one derived by Porter and Evans (2006), which applies to the case of uniform plate properties, and we found good agreement. We tested the accuracy of our solution and found it was very similar to that of Porter and Evans (2006). To obtain two-decimal places of accuracy required around 20 modes. We compared our solution method to a series of experiments performed in a two-dimensional wave tank. The agreement with the

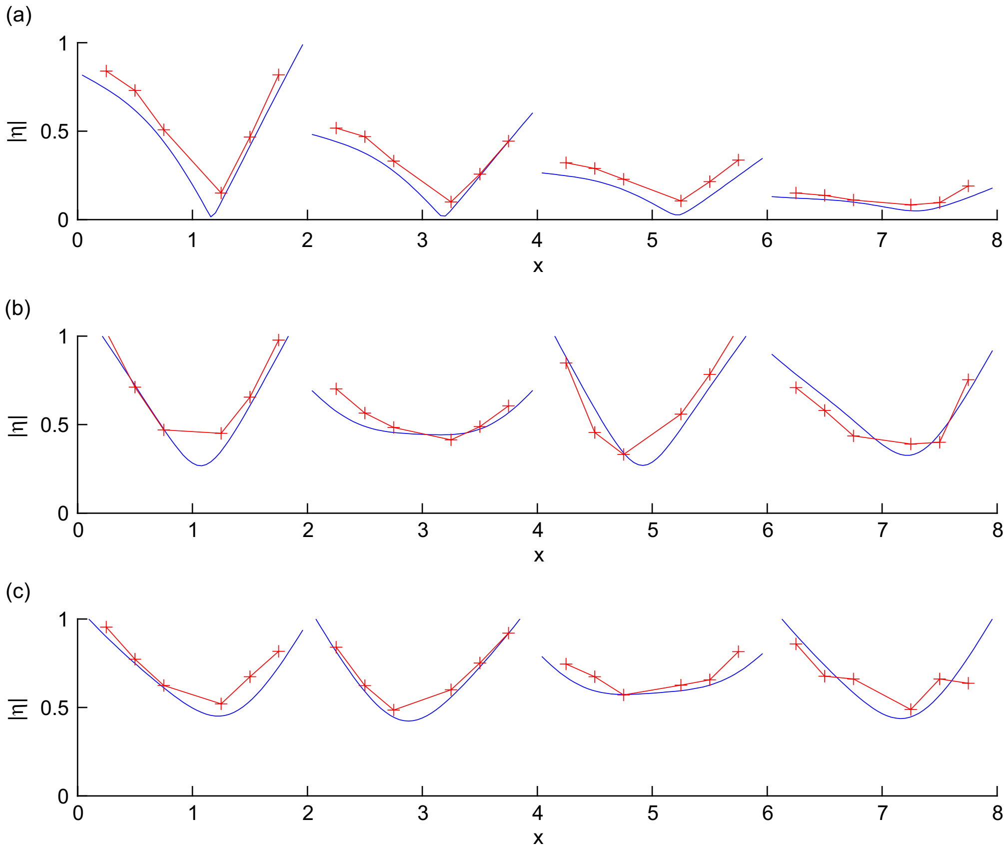

Fig. 6. As Fig. 4 except for four plates.

experiments was fairly good, and we believe we can have a high degree of confidence that our solution is correct within the expected numerical errors.

Acknowledgements

This research was supported by Marsden Grant UOO308 from the New Zealand government.

References

Balmforth, N., Craster, R., 1999. Ocean waves and ice sheets. Journal of Fluid Mechanics 395, 89–124.

Barrett, M.D., Squire, V.A., 1996. Ice-coupled wave propagation across an abrupt change in ice rigidity, density, or thickness. Journal of Geophysical Research 101, 20825–20832.

Billingham, J., King, A.C., 2000. Wave Motion. Cambridge University Press, Cambridge.

Chakrabarti, A., 2000. On the solution of the problem of scattering of surface-water waves by the edge of an ice cover. Proceedings of the Royal Society of London, Series A 456, 1087–1099.

Chung, H., Fox, C., 2002. Calculation of wave-ice interaction using the Wiener–Hopf technique. New Zealand Journal of Mathematics 31, 1–18.

Chung, H., Linton, C.M., 2005. Reflection and transmission of waves across a gap between two semi-infinite elastic plates on water. Quarterly Journal of Mechanics and Applied Mathematics 58, 1–15.

Evans, D., Davies, T., 1968. Wave-ice interaction. Technical Report 1313, Stevens Institute of Technology, NJ, USA.

Evans, D., Porter, R., 2003. Wave scattering by narrow cracks in ice sheets floating on water of finite depth. Journal of Fluid Mechanics 484, 143–165.

Fox, C., Squire, V.A., 1994. On the oblique reflexion and transmission of ocean waves at shore fast sea ice. Philosophical Transactions of the Royal Society of London, Series A 347, 185–218.

Hermans, A.J., 2003. Interaction of free-surface waves with a floating dock. Journal of Engineering Mathematics 45, 39–53.

Hermans, A.J., 2004. Interaction of free-surface waves with floating flexible strips. Journal of Engineering Mathematics 49, 133–147.

Kashiwagi, M., 2000. Research on hydroelastic response of vlfs: recent progress and future work. International Journal of Offshore and Polar Engineering 10, 81–90.

Kouzov, D., 1963. Diffraction of a plane hydro-elastic wave on the boundary of two elastic plates (in Russian). Journal of Applied Mathematics and Mechanics (Russian) 27, 541–546.

Linton, C.M., McIver, P., 2001. Handbook of Mathematical Techniques for Wave/Structure Interactions. Chapman & Hall, CRC, New York, NY.

Porter, R., Evans, D.V., 2006. Scattering of flexural waves by multiple narrow cracks in ice sheets floating on water. Wave Motion 43 (5), 425–443.

Sahoo, T., Yip, T.L., Chwang, A.T., 2001. Scattering of surface waves by a semi-infinite floating elastic plate. Physics of Fluids 13, 3215–3222.

Sakai, S., Hanai, K., 2002. Empirical formula of dispersion relation of waves in sea ice. In: Ice in the environment: Proceedings of the 16th IAHR International Symposium on Ice, Dunedin, New Zealand, pp. 327–335.

Squire, V.A., Dixon, A.W., 2000. An analytic model for wave propagation across a crack in an ice sheet. International Journal of Offshore Polar Engineering 10, 173–176.

Squire, V.A., Dixon, A.W., 2001. How a region of cracked sea ice affects ice-coupled wave propagation. Annals of Glaciology 33, 327–332.

Squire, V.A., Duggan, J.P., Wadhams, P., Rottier, P.J., Liu, A.J., 1995. Of ocean waves and sea ice. Annual Review of Fluid Mechanics 27, 115–168.

Stoker, J.J., 1957. Water Waves: The Mathematical Theory with Applications. Interscience, New York.

Teng, B., Cheng, L., Liu, S.X., Li, F.J., 2001. Modified eigenfunction expansion methods for interaction of water waves with a semi-infinite elastic plate. Applied Ocean Research 23, 357–368.

Tkacheva, L., 2001. Surface wave diffraction on a floating elastic plate. Fluid Dynamics 36, 776–789.

Wadhams, P., 2000. Ice in the Ocean. Gordon and Breach Science, New York, NY.

Wang, C.D., Meylan, M.H., 2004. A higher-order-coupled boundary element and finite element method for the wave forcing of a floating elastic plate. Journal of Fluids and Structures 19, 557–572.

Watanabe, E., Utsunomiya, T., Wang, C., 2004. Hydroelastic analysis of pontoon-type vlfs: a literature survey. Engineering Structures 26, 245–256.

Williams, T.D., Squire, V.A., 2002. Wave propagation across an oblique crack in an ice sheet. International Journal of Offshore Polar Engineering 12, 157–162.